Corrigendum to "Mare basalt meteorites, magnesian-suite rocks and KREEP reveal loss of zinc during and after lunar formation" [Earth Planet. Sci. Lett. 531 (2020) 115998]

James M.D. Day, Elishevah M.M.E. van Kooten, Beda Hofmann, Frédéric Moynier

HAL Id: insu-02916147
https://insu.hal.science/insu-02916147

Submitted on 7 Mar 2022

Mare basalt meteorites, magnesian-suite rocks and KREEP reveal loss of zinc during and after lunar formation

James M.D Day[1,2*], Elishevah M.M.E. van Kooten[2], Beda A. Hofmann[3], Frederic Moynier[2]

[1]Scripps Institution of Oceanography, University of California San Diego, La Jolla, CA 92093-0244, USA

[2] Université de Paris, Institut de Physique du Globe de Paris, CNRS UMR 7154, Paris, France

[3]Naturhistorisches Museum Bern, Bernastrasse 15, CH-3005 Bern, Switzerland.

*Corresponding author: jmdday@ucsd.edu

Abstract: 369

Total Text: 6009

Figures: 7

Tables: 2

Supplementary Tables: 2

Abstract

29   Isotopic compositions of reservoirs in the Moon can be constrained from analysis of rocks

30   generated during lunar magmatic differentiation. Mare basalts sample the largest lunar mantle

31   volume, from olivine- and pyroxene-rich cumulates, whereas ferroan anorthosites and magnesian-

32   suite rocks represent early crustal materials. Incompatible element enriched rocks, known as

33   'KREEP,' probably preserve the last highly differentiated melts. Here we show that mare basalts,

34   including Apollo samples and meteorites, have remarkably consistent δ^{66}Zn values (+1.4 ±0.2‰)

35   and Zn abundances (1.5 ±0.4 ppm). Analyses of magnesian-suite rocks show them to be

36   characterized by even heavier δ^{66}Zn values (2.5 to 9.3‰) and low Zn concentrations. KREEP-rich

37   impact melt breccia Sayh al Uhaymir 169 has a nearly identical Zn composition to mare basalts

38   (δ^{66}Zn = 1.3‰) and a low Zn abundance (0.5 ppm). Much of this variation can be explained

39   through progressive depletion of Zn and preferential loss of the light isotopes in response to

40   evaporative fractionation processes during a lunar magma ocean. Samples with isotopically light

41   Zn can be explained by either direct condensation or mixing and contamination processes at the

42   lunar surface. The δ^{66}Zn of Sayh al Uhaymir 169 is probably compromised by mixing processes

43   of KREEP with mafic components. Correlations of Zn with Cl isotopes suggests that the urKREEP

44   reservoir should be isotopically heavy with respect to Zn, like magnesian-suite rocks. Current

45   models to explain how and when Zn and other volatile elements were lost from the Moon include

46   *nebular processes*, prior to lunar formation, and *planetary processes*, either during giant impact,

47   or magmatic differentiation. Our results provide unambiguous evidence for the latter process.

48   Notwithstanding, with the currently available volatile stable isotope datasets, it is currently

49   difficult to discount if the Moon lost its volatiles relative to Earth either during giant impact or

50   exclusively from later magmatic differentiation. If the Moon did begin initially volatile-depleted,

51   then the mare basalt δ^{66}Zn value likely preserves the signature, and the Moon lost 96% of its Zn

52 inventory relative to Earth and was also characterized by isotopically heavy Cl (δ^{37}Cl = $\geq$8‰).

53 Alternative loss mechanisms, including erosive impact removing a steam atmosphere need to be

54 examined in detail, but *nebular processes* of volatile loss do not appear necessary to explain lunar

55 and terrestrial volatile inventories.

56

57

58

59

60 **1. Introduction**

61 Compared with Earth, the Moon is poor in volatile compounds (e.g., H_2O, CO_2) and elements

62 (e.g., K, Na, Cl, Zn, Rb, Sn). Comparison of volatile element data for these planetary bodies shows

63 that the Moon has lower ratios of element pairs that behave similarly during igneous processes but

64 have a more volatile numerator over denominator, including K/U and Rb/Sr (e.g., Wolf & Anders,

65 1980; Jones & Palme, 2000; O'Neill and Palme 2008; Day & Moynier, 2014). The extent of

66 volatile depletion, however, remains an open question. At one extreme, moderately volatile

67 elements are depleted by a factor of ten or more (O'Neill, 1991; Albarede et al., 2015), whereas

68 melt inclusions within olivine grains from the Apollo 74220 pyroclastic glass indicate that the

69 Moon may have as much water as Earth's depleted upper mantle (Hauri et al., 2011; Ni et al.,

70 2019). For the moderately volatile elements, defined by their nebular condensation temperatures

71 intermediate between 'common' silicate minerals (forsterite, enstatite) and troilite (Lodders,

72 2003), stable isotope ratios are fractionated by evaporation/condensation processes (e.g., Herzog

73 et al. 2009; Sharp et al., 2010; Paniello et al., 2012a; Kato et al., 2015; Boyce et al., 2015; Wang

74   & Jacobsen, 2016; Day et al., 2017a; 2019; Kato & Moynier, 2017; Pringle & Moynier, 2017;

75   Wang et al., 2019).

76

77   While the extent of volatile depletion in the Moon is an important question, how and when

78   volatile element depletion occurred may be even more critical. This is because the extent of volatile

79   depletion is dependent on how and when the process took place, which has 'planet-wide'

80   consequences. As noted previously (O'Neill and Palme 2008; Day & Moynier, 2014), at least two

81   phases of volatile depletion occurred during Solar System formation. The first was in the solar

82   nebula (*nebular depletion*), prior to or during the formation of the first solids. Partial or exclusive

83   loss of volatiles from the Moon has been proposed in this way (Humayun & Clayton, 1995; Taylor

84   el al., 2006). The second volatile depletion event, or series of events, is associated with

85   planetesimal and planet formation (*planetary depletion*). Within planetary depletion, there are

86   several avenues for volatile loss, focused around melting either during collisional events (Paniello

87   et al., 2012a; Kato & Moynier, 2017; Pringle & Moynier, 2017), or during differentiation of the

88   planets or planetesimals (Sharp et al., 2010; Kato et al., 2015; Boyce et al., 2015; Dhaliwal et al.,

89   2018).

90

91   One of the best-studied moderately volatile elements for examining volatile loss from the

92   Moon is zinc. Zinc has five stable isotopes, ^{64}Zn (48.6%), ^{66}Zn (27.9%), ^{67}Zn (4.1%), ^{68}Zn (18.8%)

93   and ^{70}Zn (0.6%) and the $^{66}Zn/^{64}Zn$ value is typically reported as the delta-notation ($\delta^{66}Zn =$

94    $([(^{66}Zn/^{64}Zn)_{sample}/(^{66}Zn/^{64}Zn)_{standard}]-1) \times 1000$) relative to the 'Lyon' Zn standard, JMC 3–0749

95   L (see Moynier et al., 2017). Zinc is moderately volatile with a low 50% nebular condensation

96   temperature (~700K) and a low bond-bond energy (e.g., Lodders, 2003; Albarède et al., 2015).

97   Mass-dependent stable isotopic fractionation of an element occurs during any exchange reaction

98   and is due to the difference in vibrational energy of the bonds formed by the different isotopes at

99   equilibrium or to the difference of motions of the isotopes under kinetic conditions (e.g., Urey,

100   1947). Zinc has been measured in partial melt products from the lunar interior as mare basalts and

101   bulk pyroclastic glass beads, some ferroan anorthosites (FAN) that are considered to make up the

102   crust, and a few magnesian-suite (MGS) rocks, which are thought to be intrusions within the crust.

103   Data from these samples has revealed a range of $\delta^{66}Zn$ values in lunar samples, from -13.7‰ to

104   +6.4‰, which have been interpreted to reflect the various processes of volatile loss and

105   condensation, largely due to differentiation processes (Moynier et al., 2006; Herzog et al., 2009;

106   Paniello et al., 2012a; Kato et al., 2015; Day et al., 2017a).

107

108   There are some restrictions in the existing lunar Zn isotope dataset that limits interpretation of

109   how, when and to what extent volatile depletion occurred in the Moon. First, only two MGS rocks

110   have been examined (dunite 72415 and norite 77215), and they both exhibit heavy $\delta^{66}Zn$ values

111   (Kato et al., 2015), making analysis of further samples to examine whether this is a ubiquitous

112   signature of the MGS important. Alternatively, it is possible that the MGS could show similar

113   ranges in $\delta^{66}Zn$ to the FAN (Kato et al., 2015). Second, Apollo 11, 12, 15 and 17 mare basalts have

114   been examined from the Moon, but these are all near-side samples from a restricted area. Mare

115   basalt meteorites are considered to come from different regions of the Moon compared with the

116   Apollo samples (e.g., Korotev, 2005), so analysis of these samples is important for assessing the

117   likelihood of homogeneity of $\delta^{66}Zn$ in lunar mantle source regions. Finally, no potassium-rare

118   earth element-phosphorous enriched samples (KREEP) have been examined for Zn isotopes. This

119   is an important lunar reservoir, as it represents the dregs of magmatic differentiation, likely from

120   a global magma ocean (Warren & Wasson, 1979). The δ^{66}Zn composition of KREEP would

121   therefore constrain models of volatile loss during magma ocean crystallization processes. In this

122   study, we take advantage of a new Zn isotopic method that decreases the required sample size by

123   a factor of approximately ten to analyze the isotope and abundance data for four MGS rocks (15445

124   cataclastic anorthositic norite [CAN] clast, 15455 'B' norite clast, 78235 shocked norite, 76535

125   troctolite), four low-Ti (<4 wt.% TiO_2) mare basalt meteorites (La Paz 02205, Northwest Africa

126   [NWA] 8632, NWA 479 and NWA 4734), as well as the first reported data on a KREEP-rich

127   sample; the impact melt breccia of Sayh al Uhaymir [SaU] 169. With these data, we examine the

128   loss of volatile Zn during processes acting prior to and during lunar formation.

129

130   **2.   Methods**

131   Aliquots of powdered samples (50 to 250 mg) were digested in a mixture of ultra-pure

132   HF/HNO_3 in Teflon beakers for 48 hours on a hotplate at 140°C. The samples were then dried

133   down and Aqua Regia was added to dissolve the aliquots for another 24 hours on the hotplate. Zinc

134   purification was achieved using an improved and miniaturized anion-exchange chromatography

135   method, with a recovery of 99.99% (see Van Kooten & Moynier, 2019 for details). Samples (5 mg

136   aliquots of total sample solutions) were loaded in 1.5N HBr on 0.1 ml AG-1X8 (200-400 mesh)

137   ion-exchange columns and Zn was collected in 0.5N HNO_3. This purification step was repeated to

138   ensure purification of the Zn fraction. The procedural blank measured with samples was 0.2 ng,

139   and generally represents less than 4% of total measured Zn for samples, which was typically 5-10

140   ng (Van Kooten & Moynier, 2019). Zinc isotopic compositions were measured on the *Thermo*

141   *Fischer* Neptune Plus multi collector-inductively coupled plasma-mass spectrometer housed at the

142   Institut de Physique du Globe, Paris. The Faraday cups were positioned to collect ions on the

143   masses 62, 63, 64, 65, 66, 67 and 68. Possible ^{64}Ni isobaric interferences were controlled and

144   corrected by measuring the intensity of the ^{62}Ni peak. A solution containing 10 ppb Zn in 0.1 M

145   HNO$_3$ was prepared for isotopic analysis. Isotopic ratios of Zn in all samples were analyzed using

146   an Apex IR introduction system, combined with a 100 µl/min PFA nebulizer. One block of 30

147   ratios, in which the integration time of 1 scan was 8.3 seconds, was measured for each sample.

148   The background was corrected by subtracting the on-peak zero intensities from a blank solution.

149   The instrumental mass bias was corrected by bracketing each of the samples with standards.

150

151   **3. Results**

152   Zinc isotope and abundance data for mare basalt meteorites (La Paz 02205, Northwest Africa

153   [NWA] 479, NWA 4734 and NWA 8632) spans a remarkably limited range, with 0.59 ±0.01 ppm

154   Zn and δ^{66}Zn of 1.23 ±0.05‰ (**Tables 1** and **2**). These values are more restricted than the range of

155   zinc abundance and isotopic compositions for Apollo mare basalts (δ^{66}Zn = +1.9 to -5.4‰; Zn =

156   0.6 to 12.1 ppm), although mare basalts typically fall within a restricted range of δ^{66}Zn

157   compositions (**Figure 1**). Compared with bulk pyroclastic glass bead data, the Apollo mare basalts

158   and mare basalt meteorites are typically isotopically heavier with respect to Zn and have lower

159   abundances.

160

161   The Apollo magnesian-suite (MGS) rocks span a limited range of Zn concentrations (0.42 to

162   1.36 ppm), and are all isotopically heavy (δ^{66}Zn = 2.46 to 9.27‰), confirming previous data

163   showing that crustal rocks have the heaviest isotope compositions of Zn of all lunar igneous rocks

164   (Kato et al., 2015). Similarly, high δ^{66}Zn has been measured in ferroan anorthosite 15415, with the

165   other FAN samples that have been measured being isotopically light (**Fig. 1**). The MGS rocks

166   examined in this study have been shown to be 'pristine', or free from impactor contamination

167   (Gros et al., 1976; Warren et al., 1980; Day et al., 2010), despite the evidence for cataclasis in

168   some MGS rocks (15445, as well as 77215 and 74215). The degree of shock and cataclasis of

169   samples is not correlated with either Zn concentration or isotopic composition.

170

171   We analyzed a portion of the 3.91 ± 0.01 Ga mafic impact melt breccia lithology of Sayh al

172   Uhaymir (SaU) 169 (Gnos et al., 2004). The ejection origin of this meteorite on the Moon has been

173   attributed to the Procellarum KREEP terrane based on enrichments of Th (32.7 ppm), U (8.6 ppm)

174   and K_2O (0.54 wt.%) within it, and it is the most KREEP-rich lunar sample examined to date (Gnos

175   et al., 2004). Our analysis of Zn (0.47 ppm) and δ^{66}Zn ($1.30 \pm 0.04\%o$) are essentially identical to

176   values obtained for the lunar mare basalt meteorites.

177

178   **4.   Discussion**

179   *4.1   Evaporation, condensation, mixing and contamination at the lunar surface*

180   Lunar materials from the Apollo missions and as meteorites have been shown to form from the

181   same silicate reservoirs based on stable isotopes of refractory major rock-forming elements (e.g.,

182   O, Mg, Si, Fe; Spicuzza et al., 2007: Liu et el., 2010; Armytage et al., 2012; Sossi & Moynier,

183   2017; Sedaghatpour & Jacobsen, 2019). For moderately volatile elements like zinc, the isotopic

184   compositions of lunar crustal samples reflect effects of evaporation, condensation, mixing and

185   contamination at the lunar surface (Moynier et al., 2006; Herzog et al., 2009; Paniello et al., 2012a;

186   Kato et al., 2015; Day et al., 2017a), as well as the Zn-bearing phases present in samples. For the

187   MGS rocks and FAN 15415, evaporation of isotopically light zinc from their parental melts that

188   exceeded those for mare basalt parental melts is required to explain both the low Zn contents and

189   high δ^{66}Zn (>2.5‰) of these samples. This process differs from that which formed the Zn-rich

190   (>10 ppm) regolith and regolith breccias, where impact gardening and spallation of isotopically

191   light Zn occurred over >100 Ma in the lunar surface environment (Moynier et al. 2006; Herzog et

192   al., 2009) (**Fig. 2**). Prior work has shown that evaporation processes during a magma ocean

193   operating throughout much/all of the Moon offers the most likely explanation for variable Zn (and

194   other volatile element) losses in magmatically-derived rocks (e.g., Day & Moynier, 2014; Boyce

195   et al., 2015; Dhaliwal et al., 2018).

196

197   Modelling the effect of zinc isotope evaporation is possible through empirically derived

198   fractionation factors that are closer to unity (>0.999) than theoretical values (Day et al., 2017b;

199   Wimpenny et al., 2019). Acknowledging that there was no single mantle source for MGS rocks,

200   we take the approach of modelling evaporation processes in them as a unified process, with an

201   initial starting composition of 30 ppm Zn and δ^{66}Zn = 1.25‰. The δ^{66}Zn was chosen to reflect a

202   source similar to the mare basalt source (e.g., Paniello et al., 2012a). The high content of Zn in the

203   source of MGS rocks is due to the progressive Zn enrichment that counters loss through

204   evaporation and that was likely to have occurred in a magma ocean (Dhaliwal et al., 2018). The

205   bulk partition coefficient for Zn under terrestrial conditions is typically approximated as close to

206   unity ($D_{mantle-melt}\sim 1$), with limited fractionation of Zn isotopes during fractional crystallization

207   (e.g., Chen et al., 2013; Doucet et al., 2016), indicating that MGS rocks should derive from a

208   mantle reservoir that is more Zn-rich than for the mare basalts. The low Zn measured in mare

209 basalts (1-2 ppm) are consistent with previous estimates of a bulk Moon Zn content (~2 ppm;

210 O'Neill, 1991). The choice of Zn concentration in the source is difficult to estimate without

211 knowing the lunar bulk partition coefficient, but any concentration between ~10 and 30 ppm for

212 the MGS parental melts leads to broadly similar outcomes to the models shown in **Figure 2**.

213 However, higher estimated concentrations in the source (>30 ppm) or lower $\delta^{66}Zn$ (e.g., 0.3‰ as

214 in chondrites or Earth) require lower fractionation factors and a poorer fit to the data.

215

216   The variable $\delta^{66}Zn$ of MGS rocks implies inhomogeneous evaporative loss of zinc amongst

217 these samples, either reflecting different extents of evaporation, varying efficiency of evaporative

218 fractionation, or heterogeneous initial Zn in their parental sources. These results are consistent

219 with more than one mantle source of MGS samples, and for the possibility of mixing between

220 early LMO olivine, plagioclase and KREEP reservoirs (e.g., Shearer et al., 2015). The variability

221 in Zn isotopic compositions in the MGS rocks and in FAN 15415 are most consistent with

222 inheritance of these signatures from variable evaporative loss during the late stages of a magma

223 ocean, and after formation of the mare basalt source reservoirs, where higher $\delta^{66}Zn$ values are

224 expected provided that the resultant evaporated Zn condensates could be effectively lost (Dhaliwal

225 et al., 2018). The CAN clast of 15455 (9.3‰), cataclastic dunite 72415 (6.3‰) and 15415 (4.2‰)

226 would represent products from the most extremely fractionated and latest crystallized melts in this

227 model.

228

229   Some of the isotopically light condensate Zn from lunar degassing remains on the lunar surface

230 today. Analysis of the 'Rusty Rock' 66095 has illustrated how magmatic outgassing, during

231   impact-related or volcanic events on the Moon, led to significant condensation of isotopically light

232   vapors into the impact melt breccia (Day et al., 2017a; 2019). Similarly, volatile condensation onto

233   the lunar surface can explain how late-stage differentiates in the Moon evolved to higher δ^{66}Zn

234   than mare basalt sources. Modelled condensate compositions match δ^{66}Zn values measured for the

235   Zn-rich 'Rusty Rock' 66095 (**Fig. 2**). Mixing of evaporated reservoirs and condensates on the

236   lunar surface also matches trends observed in δ^{66}Zn and Zn content for the FAN, further

237   reinforcing the concept that volatile loss during the magma ocean was facilitated by the formation

238   of the lunar crust. Stabilization and thickening of the cooling lunar crust would inevitably have led

239   to the formation of a sink for condensate volatiles, separating them from the magma ocean, and

240   enabled rapid depletion of volatile contents in the hot molten rocks, without the requirement for

241   other volatile-loss mechanisms.

242

243   *4.2   Zinc isotope composition of mare basalt sources*

244   With five exceptions (10017, 12005, 12018, 14053, 15016), mare basalts have a range of δ^{66}Zn

245   values from 0.8 to 1.9‰ (**Fig. 3**). As originally suggested by Paniello et al. (2012a) and quantified

246   in the presented models, mixing and contamination from isotopically light Zn on the lunar surface

247   explains the isotopically light basalts reported previously. Mixing and contamination of between

248   10 and 50% condensate Zn matching that measured in 66095 provides a good approximation for

249   the Zn compositions of these anomalous mare basalts. These results are supported by leaching

250   experiments on 14053 which show that the silicate fraction of the sample was identical to the

251   majority of mare basalts at ~1.4‰ (Day et al., 2017a). Contamination of lunar mare basalts could

252   have occurred through two mechanisms. First, Zn could have been assimilated during ascent of

253   magmas and eruption on the lunar surface, where mare basalts would be highly sensitive to

254   assimilation of volatile phases due to low magmatic Zn contents (<2 ppm) versus high contents in

255   condensates (e.g., 300 ppm in 66095). Second, Zn addition could have occurred through partial

256   condensation directly onto samples during or after they had crystallized. This latter process is

257   possibly analogous to the pyroclastic glass beads 15426, 74001 and 74220, that experienced

258   directed condensation onto the bead surfaces, during or after their formation. The surface areas of

259   the beads, combined with evidence for Zn phases on the exteriors of the beads (Ma & Liu, 2019)

260   and high Zn abundances correlated to these outer surfaces (e.g. Herzog et al. 2009), implies that

261   the beads were effective 'traps' of condensate volatile species.

262

263   It has been suggested that volatile loss of Cl occurred during eruption and crystallization of

264   lava flows on the lunar surface (Sharp et al., 2010). To examine whether Zn isotopes were

265   fractionated during eruption, we compare mare basalt δ^{66}Zn values with petrological proxies of

266   outgassing and lava-flow differentiation. We compare texture, presence or absence of vesicles and

267   vugs, and bulk-rock MgO content. The presence of vesicles in basaltic rocks indicates outgassing

268   of gas species, while coarser-grained lava samples might be associated with prolonged outgassing

269   processes at the lunar surface, or relate to suites of samples from the Apollo landing sites

270   originating from the same lava flow. Magnesium oxide (MgO) is an indicator of differentiation, as

271   this compound is compatible in early crystallizing silicate mineral phases, including olivine,

272   orthopyroxene and clinopyroxene. Relationships of MgO with Zn and δ^{66}Zn, therefore, might be

273   expected to relate to outgassing prior to, during and after eruption during lava flow differentiation

274   processes in Apollo mare basalt suites (e.g., Rhodes & Hubbard, 1973; Neal & Taylor, 1992;

275   Schnare et al., 2008). While some mare basalt samples, specifically some of the mare basalt

276   meteorites, have quantitative textural data associated with them (Day & Taylor, 2007), textural

277   descriptions in the literature for Apollo mare basalts are often qualitative, being described as fine,

278   medium or coarse grained. Mare basalt samples also have a range of textures from porphyritic

279   (e.g., 15058, 15499), to poikilitic (e.g., 70135), ophitic or aphanitic. Acknowledging current

280   petrological complexities, we defined samples where average grain sizes are reported as <0.5 mm

281   as fine-grained, samples with grain sizes of >2 mm as coarse grained, and intermediate samples as

282   medium-grained (**Table S1**).

283

284   Comparison of $\delta^{66}Zn$ with presence or absence of vesicles shows that they are not correlated

285   (**Fig. 4**). Mare basalts with the most negative $\delta^{66}Zn$ (<-1‰) are medium to fine-grained, but

286   otherwise there is no relationship of grain-size with mare basalt $\delta^{66}Zn$ values. Nor do the Zn

287   isotope compositions track changes with magmatic differentiation. Low-Ti mare basalts have

288   uniformly low Zn abundances (<2 ppm) and there is no correlation between MgO and $\delta^{66}Zn$ (**Fig.**

289   **5**). High-Ti basalts show a wide range of $\delta^{66}Zn$ and Zn content for a limited range of MgO, likely

290   due to higher compatibility of Zn within spinel and oxide phases, but otherwise no relationships

291   between $\delta^{66}Zn$ and MgO exist. While these lines of evidence do not rule out minor degassing of

292   Zn during lava flow emplacement processes, or for degassing of other volatiles, such as H or Cl,

293   they demonstrate that this is not the dominant process for $\delta^{66}Zn$ variations in mare basalts. Instead,

294   these comparisons provide evidence that the average $\delta^{66}Zn$ of mare basalts reflect that of their

295   mantle source reservoirs within the Moon, as suggested previously (Paniello et al., 2012a; Kato et

296   al., 2015). We confirm this with new mare basalt meteorite data that suggest a homogeneous mare

297   basalt mantle source reservoir for zinc. Removing the five samples with negative $\delta^{66}Zn$ from the

298 compilation, mare basalts as a whole are characterized by a $\delta^{66}Zn$ value of 1.40 ± 0.08‰ (**Table**

299 **2**). There are variations in $\delta^{66}Zn$ between high-Ti mare basalts (1.50 ± 0.15‰) and low-Ti mare

300 sources (1.37 ± 0.15‰), but any significant differences that may occur are outside current levels

301 of analytical precision.

302

303 ### *4.3   The zinc isotope composition of KREEP and relations to H and Cl*

304 The potassium-rare earth element-phosphorous enriched (KREEP) reservoir has been shown

305 to exist dominantly in the nearside Procellarum KREEP Terrane (Jolliff et al., 2000). Numerous

306 Apollo 12 and 14 samples, MGS rocks, and some mare basalt meteorites (e.g., LaPaz mare basalts)

307 have KREEP signatures and similar inter-element ratios of incompatible elements, implying a

308 single KREEP reservoir, sometimes referred to as urKREEP (Warren & Wasson, 1979). This

309 reservoir is postulated to have formed during crystallization of a lunar magma ocean, where

310 elements that are incompatible in silicate minerals (olivine, pyroxene, plagioclase) would be

311 predicted to concentrate in residual melts. Given that many moderately volatile elements and

312 compounds like water are incompatible, this reservoir should be the most volatile-rich reservoir in

313 the Moon. This appears to be the case for Cl, which is estimated to have ~28 times higher

314 abundances relative to mare basalts (Boyce et al., 2018).

315

316 To date, no pristine urKREEP sample has been discovered, and all KREEP-rich rocks have

317 Mg-numbers (atomic ratios of Mg/Mg + Fe) too high to have formed as direct late-stage magma

318 ocean products (e.g., Snyder et al., 1992). KREEP-rich rocks with high Mg-numbers can be

319 explained by the incorporation of an urKREEP signature, via mixing or contamination, into partial

320 melts from early-formed olivine and pyroxene-rich cumulate reservoirs (e.g., Warren & Wasson,

321 1979; Snyder et al., 1992; Shearer et al., 2015). The SaU 169 impact melt breccia is no exception

322 to this rule; while it is among the most KREEP-rich samples reported to date, being enriched in

323 incompatible trace elements by factors of 1.5 to 1.8 relative to the KREEP composition reported

324 by Warren & Wasson (1979), it is also Mg-rich (Mg-number = 70; Gnos et al., 2004). SaU 169

325 has similar Zn isotope and abundance systematics to mare basalts (**Table 1**); this differs from the

326 prediction that KREEP should be heavier for $\delta^{66}Zn$ based on models of magma ocean processes

327 (Dhaliwal et al., 2018). We suggest two possible reasons for this discrepancy and favor the latter

328 explanation. First, the similarity of $\delta^{66}Zn$ in KREEP compared with mare basalts could reflect no

329 change in $\delta^{66}Zn$ during magma ocean processes, contrary to models. Second, the $\delta^{66}Zn$ of SaU 169

330 is not reflective of pure urKREEP, but is rather reflective of mixing with mafic components during

331 its petrogenesis.

332

333   Boyce et al. (2015) and Barnes et al. (2016) have argued for KREEP mixing into mare basalt

334 sources to explain apatite $\delta^{37}Cl$ values, and have made this association from extrapolations with

335 MGS rocks, including 76535 and 78235, which are isotopically heavy with respect to Cl ($\delta^{37}Cl =$

336 >30‰) and that have fractionated La/Lu and La/Sm, consistent with an urKREEP signature. These

337 MGS samples also have high $\delta^{66}Zn$ (3.1 to 3.5‰), so if KREEP was partially responsible for the

338 variations in moderately volatile isotopic compositions, one might also expect to see a correlation

339 with Zn isotopes in mare basalts and a KREEP signature. Abundance ratios of La and Lu are useful

340 for assessing possible urKREEP mixing with mare basalts, because urKREEP is considered to

341 have high La (230 ppm) and Lu (7.8 ppm), with La/Lu of 29.5, versus KREEP-free mare sources

342 with lower La (1.1 ppm) and Lu (0.26 ppm) and a low La/Lu ratio (4.2) (Boyce et al., 2018). Mare

343   basalt La/Lu ratios are not correlated with Zn isotopic composition (**Table S1**), with Apollo 17

344   basalts with low La/Lu (~4) having broadly similar δ^{66}Zn to Apollo 15 basalts with the highest

345   La/Lu (~18). This result indicates that admixtures of KREEP and a mare basalt source are not

346   required to explain δ^{66}Zn values in mare basalts. Consequently, this suggests that KREEP addition

347   does not control Zn isotopic variations in mare basalts, or that KREEP has the same δ^{66}Zn value

348   to the mare basalt source.

349

350   In contrast, evidence supporting a higher δ^{66}Zn value for KREEP than that measured in SaU

351   169 comes from comparisons of Zn with H and Cl isotope compositions. Comparison of Zn with

352   Cl and H is not intuitive as H and Cl abundances tend to be measured within apatite, where they

353   can be preferentially partitioned into the mineral structure ($Ca_5[PO_4]_3[Cl,F,OH]$), whereas Zn is

354   likely sited within S-rich phases and silicate minerals in lunar rocks. Indeed, analysis of the Rusty

355   Rock, 66095, has demonstrated decoupling of Cl, Cu and Fe from Zn isotope compositions, largely

356   due to condensation effects on the sample (Day et al., 2017a; 2019). In contrast, magmatic phases

357   are likely to trap the H, Cl and Zn compositions within mare basalts and HMS rocks making

358   comparisons between these elements possible. Positively correlated relationships for Cl and Zn

359   have previously been reported for eucrite meteorites (Sarafian et al., 2017; Barrett et al., 2019).

360   This trend has been interpreted to reflect degassing of $ZnCl_2$ in an H-poor environment in the

361   eucrite parent body (4 Vesta).

362

363   We find no relationship between H and Zn isotope ratios (**Fig. 6a**). However, we note a

364   relationship of increasing δ^{37}Cl with increasing δ^{66}Zn from mare basalts to MGS rocks (**Fig. 6b**).

365   The Zn-Cl isotope lunar trend is not well-developed and is steeper than the eucrite data trend. For

366   a given Cl isotope composition, Zn isotopes are less fractionated in lunar samples than in eucrite

367   meteorites, implying possible differences in extents and style of degassing. Furthermore, for mare

368   basalts, there is a restricted range in Zn (δ^{66}Zn = 1.4‰), as well as consistently heavy Cl isotope

369   compositions (δ^{37}Cl = 8 to 15‰). KREEP impact melt breccia SaU 169 lies within this range

370   (δ^{66}Zn = 1.3‰, δ^{37}Cl = 9‰). This composition likely reflects the dominant role of a mafic

371   component in the sample, consistent with the high MgO (12.2 wt.%) and bulk composition of the

372   impact melt breccia itself (Gnos et al., 2004).

373

374   The most extremely heavy δ^{66}Zn from the Moon is for the CAN clast in 15455 (9.3‰), versus

375   for basaltic eucrite DaG 945 (13.5‰) that is the most extreme equivalent from Vesta. These

376   comparisons suggest that greater loss of Zn occurred on Vesta compared with the Moon, which

377   would confirm previous measurements of K/U and Rb/Sr ratios, and with planetary body size (Day

378   & Moynier, 2014). Estimates for maximum chlorine loss via degassing are similar for the Moon

379   and Vesta (**Fig. 6**), which makes this isotope proxy of moderately volatile element loss distinct

380   from those of δ^{66}Zn, K/U or Rb/Sr. These results suggest contrasting degassing processes for Cl

381   and Zn, with Zn loss on Vesta possibly occurring as $ZnCl_2$ (e.g., Barrett et al., 2019). The lunar

382   urKREEP composition is an important composition to measure for Zn isotopes to examine volatile

383   loss models for Moon and Vesta. Based on KREEPy impact breccia SaU 169, the KREEP reservoir

384   would have δD, δ^{37}Cl and δ^{66}Zn within the range of mare basalts, but these values are significantly

385   lower in δD and δ^{37}Cl than for the classic KREEP basalt 15382/6. Magma ocean models predict

386   urKREEP to have δ^{66}Zn higher than mare basalt sources (Dhaliwal et al., 2018). To test if KREEP

387   does have an elevated Zn isotope composition, and if degassing processes on Vesta and Moon

388   were similar, measurement of KREEP basalt 15382/6 will be critical given the high $\delta^{37}Cl$ (22

389    $\pm 8‰$; Barnes et al., 2016) of apatite grains within the sample.

390

391   ### *4.4   Early loss of Zn and Cl through crust-breaching impacts or before lunar formation?*

392   The significant difference between $\delta^{66}Zn$ values of MGS rocks and mare basalts provide

393   unequivocal evidence that Zn was lost, and its isotopes fractionated, during evaporative

394   fractionation processes on the Moon. The most likely cause of Zn loss between the formation of

395   the mare basalt sources and the crystallization of MGS rocks was during magma ocean

396   differentiation, supporting models of progressive loss of volatiles from the lunar interior during

397   magma ocean degassing (Dhaliwal et al. 2018), and the elevated $\delta^{66}Zn$ and $\delta^{35}Cl$ values in MGS

398   rocks. On the other hand, the homogenous $\delta^{66}Zn$ values of mare basalt sources suggest a large-

399   scale process for their generation, either through magma ocean processes (Kato et al., 2015;

400   Dhaliwal et al., 2018), or prior to or during the giant impact (Paniello et al., 2012a). The bulk

401   silicate Earth (BSE) value for $\delta^{66}Zn$ is between 0.16 and 0.3‰ (Chen et al., 2013; Wang et al.,

402   2017; Sossi et al., 2018), and its Zn content is estimated at 55 ppm (McDonough & Sun, 1995),

403   whereas the $\delta^{66}Zn$ and Zn content for CI chondrites are ~0.3‰ and 310 ppm (Moynier et al., 2017).

404   As mentioned previously, mare basalt sources have $\delta^{66}Zn$ of 1.40 ± 0.08‰, and Zn contents as

405   low as 1-2 ppm. At face value, the BSE is depleted by more than 80% of Zn compared with

406   chondrites, assuming it formed from similar sources, without significantly fractionating Zn

407   isotopes. Part of the BSE Zn loss can be explained by core formation as under conditions relevant

408   to Earth's core differentiation Zn is slightly siderophile and the bulk Earth may have ~ 114 ppm

409   (Mahan et al. 2017). Conversely, the reservoir of mare basalts has lost significantly more Zn (99%

410   relative to chondrites, 96% relative to Earth), and has experienced evaporative fractionation of Zn

411   isotopes, suggesting that the lunar Zn depletion is due to planetary processes.

412

413   Understanding whether the difference in Zn abundances and isotopic compositions between

414   the Moon and Earth occurred through volatile-loss of material forming the Moon in a giant impact

415   (**Fig. 7**), or whether it was wholly lost after this event during magma ocean degassing and other

416   processes on the Moon, is important for models to explain the formation of the Moon, including

417   volatile loss during a lunar 'synestia' (Lock et al., 2018), from a lunar disk (Nakajima & Stevenson,

418   2018), or from the Moon itself (Dhaliwal et al. 2018). Dhaliwal et al. (2018) showed that during

419   magma ocean processes, volatile loss could occur throughout the cooling of the magma ocean, but

420   that the volatile condensates required a loss-mechanism. The 'problem' of how to separate

421   isotopically light condensate Zn from the melt residue during magma ocean processes on the Moon

422   can be at least partially resolved by condensation onto the cooling lunar surface (Day et al., 2017a),

423   or to the Earth when the early forming Moon was at the Roche limit (Sossi et al. 2018).

424   Condensation of volatiles on the forming crust acts to effectively remove the isotopically light Zn

425   condensate and would indicate that Zn isotope fractionation might have been initially slow during

426   the early stages of lunar differentiation when early-formed crust as only semi-permanent,

427   foundering into the lunar interior. Later, as the crust became stable and permanent, rapid evolution

428   and complexity in Zn isotope compositions of crustal rocks could have occurred.

429

430   Another likely mechanism for volatile loss might include impacts to the Moon during lunar

431   magma ocean formation and after dissipation of a nascent atmosphere surrounding the Moon (**Fig.**

432   **7**), as has been suggested previously (Barnes et al., 2016). Retention of impactor mass has been

433   shown to be quite low, of the order of 20 to 30%, and large impactors striking the Moon were

434   likely to have been numerous, with as many as 300 impact basins of initial diameters of 300 km

435   or more up to ~4.1 Ga (Zhu et al., 2019). These features imply that erosive-loss of a nascent

436   atmosphere on the Moon was likely and may have occurred as many as 300 times or more between

437   the formation of the Moon and ~4.1 Ga. However, the likelihood of erosive loss of isotopically

438   light condensates from the Moon is limited for two reasons. First is the effectiveness and quantity

439   of volatile species that can be retained as a steam gas atmosphere above a molten magma ocean

440   on the Moon, prior to erosive impacts. Second, is the requirement that loss of Zn by impact erosion

441   must have affected the Moon across the entire formation of mare basalt sources, from low-Ti to

442   high-Ti compositions, during a magma ocean (**Fig. 7**). To fully investigate this problem, combined

443   modeling efforts to estimate gas contents in a lunar steam atmosphere and to examine if impact-

444   erosion can successfully remove this atmosphere are needed.

445

446   Alternatively, the homogeneity of mare basalt δ^{66}Zn values might suggest a global signature

447   of volatile element depletion inherited from the giant impact. Various studies have proposed loss

448   of moderately volatile elements (K, Rb, Ga, Sn: Wang & Jacobson, 2016; Pringle & Moynier,

449   2017; Kato & Moynier, 2017; Wang et al., 2019) prior to the formation of the Moon, but few of

450   them have been able to provide robust resolution of when volatile loss occurred, mainly due to the

451   limited number of samples and associated lunar reservoirs analyzed. Arguments have typically

452   relied on differences in the isotopic compositions of moderately volatile elements between lunar

453   and terrestrial samples. However, this approach cannot necessarily discriminate between volatile

454   element loss prior to the formation of the Moon, from nebular volatile loss processes, during giant

455   impact, or during or after the formation of the Moon.

456

457   With a large set of Zn isotope data it is possible to distinguish processes acting on volatile

458   elements *after* the formation of the Moon. The heavy $\delta^{66}Zn$ (>2.5‰) of pristine MGS and FAN

459   samples, and the light isotopic compositions of some mare basalts and FAN (<0‰) can be

460   explained by magmatic degassing and condensation of isotopically light Zn, respectively. If the

461   Moon did experience moderately volatile element loss *prior to*, or *during* its formation, then the

462   Zn isotope signature of that event would be recorded by the mare basalts at 1.4‰. In this scenario,

463   significant moderately volatile element loss and Zn isotope fractionation occurred to materials

464   forming the Moon, leading to a 1.1 to 1.2‰ difference between terrestrial $\delta^{66}Zn$ (~0.16-0.3‰;

465   Chen et al., 2013; Wang et al., 2017; Moynier et al. 2017; Sossi et al., 2018) and the composition

466   of the Moon. Without data for urKREEP to examine the maximum extents of magma ocean

467   degassing, and without collision models to examine if volatile elements could be effectively

468   stripped from the Moon during its formation, it is impossible to say with confidence if this

469   signature was inherited *prior to*, *during* or *after* the formation of the Moon. Notwithstanding, if

470   mare basalts do record the Zn isotope signature during the formation of the Moon, then it would

471   suggest that the Moon also inherited an isotopically heavy Cl ($\delta^{37}Cl$ = 8 to 15‰) signature from

472   this event.

473

474   **5. Conclusions and implications for volatile loss during moon and planet formation**

475   New data are presented for mare basalt meteorites to show that they, and Apollo mare basalts,

476   have remarkably consistent δ^{66}Zn values (+1.4 ±0.2‰) and low Zn (1.5 ±0.4 ppm) inherited from

477   their mantle sources. New analyses of magnesian-suite rocks show them to be characterized by

478   even heavier δ^{66}Zn values (2.5 to 9.3‰) and low Zn concentrations. Zinc isotope analysis of

479   KREEP impact melt sample Sayh al Uhaymir 169 shows that it has a nearly identical composition

480   to mare basalts (δ^{66}Zn = 1.3‰, 0.5 ppm [Zn]). We explain these variations through progressive

481   depletion of Zn and preferential loss of the light isotopes in response to evaporative fractionation

482   processes during lunar magmatic differentiation. Variations in δ^{66}Zn in samples to isotopically

483   light values can be explained by condensation of isotopically light Zn on the lunar surface and

484   mixing and contamination processes with magmas interacting with these surface reservoirs. The

485   δ^{66}Zn of KREEP defined by Sayh al Uhaymir 169 is likely to be compromised by mixing processes

486   with a mafic component. Correlations of Zn with Cl isotopes suggests that the KREEP reservoir

487   should also be isotopically heavy, like the magnesian-suite rocks, and analysis of 15382/15386

488   will be essential to test this hypothesis.

489

490   Current models to explain how and when Zn and other volatile elements were lost from the

491   Moon include *nebular processes*, prior to the Moon's formation, and *planetary processes*, either

492   during the formation of the Moon in a giant impact, or during magmatic differentiation. Our results

493   provide unambiguous evidence for the latter process and imply that *nebular processes* are not

494   required to explain the excessive depletion in volatile elements in the Moon relative to Earth. On

495   the other hand, with the currently available volatile stable isotope datasets, it is currently difficult

496   to say with certainty whether the Moon lost its volatiles relative to Earth either during giant impact

497   or from later magmatic differentiation. If the Moon did begin initially volatile-depleted, then the

498   mare basalt $\delta^{66}Zn$ value likely preserves that signature, in which case the Moon lost 96% of its

499   zinc inventory relative to Earth at that time and was also characterized by isotopically heavy Cl

500   ($\delta^{37/35}Cl = \geq 8\text{‰}$).

501

Acknowledgements

518

References

520   Albarède, F., Albalat, E., Lee, C.T.A., 2015. An intrinsic volatility scale relevant to the Earth and
521   Moon and the status of water in the Moon. Meteoritics & Planetary Science 50, 568-577.
522   Armytage, R.M.G., Georg, R.B., Williams, H.M., Halliday, A.N., 2012. Silicon isotopes in lunar
523   rocks: implications for the Moon's formation and the early history of the Earth. Geochimica et
524   Cosmochimica Acta, 77, 504-514.
525   Barnes, J.J., Tartèse, R., Anand, M., McCubbin, F.M., Franchi, I.A., Starkey, N.A., Russell, S.S.,
526   2014. The origin of water in the primitive Moon as revealed by the lunar highlands samples.
527   Earth and Planetary Science Letters, 390, 244-252.
528   Barnes, J.J., Tartese, R., Anand, M., McCubbin, F.M., Neal, C.R., Franchi, I.A., 2016. Early
529   degassing of lunar urKREEP by crust-breaching impact(s). Earth and Planetary Science Letters,
530   447, 84-94.
531   Barnes, J.J., Franchi, I.A., McCubbin, F.M., Anand, M., 2018. Multiple reservoirs of volatiles in
532   the Moon revealed by the isotopic composition of chlorine in lunar basalts. Geochimica et
533   Cosmochimica Acta, https://doi.org/10.1016/j.gca.2018.12.032.
534   Barrett, TJ., Barnes, J.J., Anand, M., Franchi, I.A., Greenwood, R.C., Charlier, B.L.A., Zhao, X.,
535   Moynier, F., Grady, M.M., 2019. Investigating magmatic processes in the early Solar System

using the Cl isotopic systematics of eucrites. Geochimica et Cosmochimica Acta, https://doi.org/10.1016/j.gca.2019.06.024

Boyce, J.W., Treiman, A.H., Guan, Y., Ma, C., Eiler, J.M., Gross, J., Greenwood, J.P., Stolper, E.M., 2015. The chlorine isotope fingerprint of the lunar magma ocean. Science Advances, 1, e1500380.

Boyce, J.W., Kanee, S.A., McCubbin, F.M., Barnes, J.J., Bricker, H., Treiman, A.H., 2018. Early loss, fractionation, and redistribution of chlorine in the Moon as revealed by the low-Ti lunar mare basalt suite. Earth and Planetary Science Letters, 500, 205-214.

Chen, H., Savage, P.S., Teng, F.-Z., Helz, R.T., Moynier, F., 2013. Zinc isotopic fractionation during magmatic differentiation and the isotopic composition of the bulk Earth. Earth and Planetary Science Letters, 369-370, 34-42.

Chen, Y., Zhang, Y., Liu, Y., Guan, Y., Eiler, J., Stolper, E.M., 2015. Water, fluorine, and sulfur concentrations in the lunar mantle. Earth and Planetary Science Letters 427, 37-46.

Day, J.M.D., Taylor, L.A., 2007. On the structure of mare basalt lava flows from textural analysis of the LaPaz Icefield and Northwest Africa 032 lunar meteorites. Meteoritics & Planetary Science, 42, 3-17.

Day, J.M.D., Moynier, F., 2014. Evaporative fractionation of volatile stable isotopes and their bearing on the origin of the Moon. Phil. Trans. Royal Soc. London A, 372(2024), 20130259.

Day, J.M.D., Walker, R.J., James, O.B., Puchtel, I.S., 2010. Osmium isotope and highly siderophile element systematics of the lunar crust. Earth and Planetary Science Letters, 289, 595-605.

Day, J.M.D., Moynier, F., Shearer, C.K. 2017a. Late-stage magmatic outgassing from a volatile-depleted Moon. Proceedings of the National Academy of Sciences, 114, 9457-9551.

Day, J.M.D., Moynier, F., Meshik, A.P., Pradivtseva, O.V. and Petit, D.R., 2017b. Evaporative fractionation of zinc during the first nuclear detonation. Science advances, 3, e1602668.

Day, J.M.D., Sossi, P.A., Shearer, C.K., Moynier, F., 2019. Volatile distributions in and on the Moon revealed by Cu and Fe isotopes in the 'Rusty Rock' 66095. Geochimica et Cosmochimica Acta. https://doi.org/10.1016/j.gca.2019.02.036

Dhaliwal, J.K., Day, J.M.D., Moynier, F., 2018. Volatile element loss during planetary magma ocean phases. Icarus, 300, 249-260.

Doucet, L.S., Mattielli, N., Ionov, D.A., Debouge, W., Golovin, A.V., 2016. Zn isotopic heterogeneity in the mantle: A melting control? Earth and Planetary Science Letters, 451, 232-240.

Gnos E., Hofmann B.A., Al-Kathiri A., Lorenzetti S., Eugster O., Whitehouse M.J., Villa I., Jull A.J.T., Eikenberg J., Spettel B., Krähenbühl U., Franchi I.A., Greenwood R.C. (2004) Pinpointing the source of a lunar meteorite: Implications for the evolution of the Moon. Science 305, 657-659.

Gros, J., Takahashi, H., Hertogen, J., Morgan, J.W., Anders, E., 1976. Composition of the projectiles that bombarded the lunar highlands. Lunar and Planetary Science Conference Proceedings, 7, 2403-2425.

Hauri, E. H.,Weinreich, T., Saal, A., Rutherford, M., Van Orman, J. A., 2011. High Pre-Eruptive Water Contents Preserved in Lunar Melt Inclusions. Science, 333, 213-215.

Herzog, G.F., Moynier, F., Albarède, F., Berezhnoy, A.A., 2009. Isotopic and elemental abundances of copper and zinc in lunar samples, Zagami, Pele's hairs, and a terrestrial basalt. Geochimica et Cosmochimica Acta 73, 5884-5904.

581   Hui, H., Guan, Y., Chen, Y., Peslier, A.H., Zhang, Y., Liu, Y., Flemming, R.L., Rossman, G.R.,
582   Eiler, J.M., Neal, C.R., Osinski, G.R., 2017. A heterogeneous lunar interior for hydrogen
583   isotopes as revealed by the lunar highlands samples. Earth and Planetary Science Letters, 473,
584   14-23.
585   Humayun, M., Clayton, R.N., 1995. Potassium isotope geochemistry: genetic implications of
586   volatile element depletion. Geochimica et Cosmochimica Acta, 59, 2115-2130.
587   Jolliff, B.L., Gillis, J.J., Haskin, L.A., Korotev, R.L., Wieczorek, M.A., 2000. Major lunar crustal
588   terranes: Surface expressions and crust-mantle origins. Journal of Geophysical Research:
589   Planets, 105, 4197-4216.
590   Jones, J.H., Palme, H., 2000. Geochemical constraints on the origin of the Earth and Moon. In:
591   Canup, R.M., Righter, K. (Eds.) Origin of the Earth and Moon, University of Arizona Press,
592   Tucson, 555 pp., p.197-216.
593   Kato, C., Moynier, F., Valdes, M.C., Dhaliwal, J.K., Day, J.M.D., 2015. Extensive volatile loss
594   during formation and differentiation of the Moon. Nature communications, 6, 7617.
595   Kato, C., Moynier, F., 2017. Gallium isotopic evidence for extensive volatile loss from the Moon
596   during its formation. Science advances, 3, e1700571.
597   Korotev R. L., 2005. Lunar geochemistry as told by lunar meteorites. Chemie der Erde 65, 297-
598   346.
599   Liu, Y., Spicuzza, M.J., Craddock, P.R., Day, J.M.D., Valley, J.W., Dauphas, N., Taylor, L.A.,
600   2010. Oxygen and iron isotope constraints on near-surface fractionation effects and the
601   composition of lunar mare basalt source regions. Geochimica et Cosmochimica Acta, 74, 6249-
602   6262.
603   Lock, S.J., Stewart, S.T., Petaev, M.I., Leinhardt, Z., Mace, M.T., Jacobsen, S.B. and Cuk, M.,
604   2018. The origin of the Moon within a terrestrial synestia. Journal of Geophysical Research:
605   Planets, 123, 910-951.
606   Lodders, K., 2003. Solar System abundances and condensation temperatures of the elements.
607   Astrophysical Journal, 591, 1220-1247.
608   Ma, C., Liu, Y., 2019. Discovery of a zinc-rich mineral on the surface of lunar orange pyroclastic
609   beads. American Mineralogist, 104, 447-452.
610   McCubbin, F.M., Kaaden, K.E.V., Tartese, R., Klima, R.L., Liu, Y., Mortimer, J., Barnes, J.J.,
611   Shearer, C.K., Treiman, A.H., Lawrence, D.J., Elardo, S.M., 2015. Magmatic volatiles (H, C,
612   N, F, S, Cl) in the lunar mantle, crust, and regolith: Abundances, distributions, processes, and
613   reservoirs. American Mineralogist 100, 1668-1707.
614   McDonough, W.F., Sun, S.-S., 1995. The composition of the Earth. Chemical Geology, 120, 223-
615   254.
616   Moynier, F., Albarède, F., Herzog, G.F. 2006. Isotopic composition of zinc, copper, and iron in
617   lunar samples. Geochimica et Cosmochimica Acta 70, 6103–6117.
618   Moynier, F., Vance, D., Fujii, T., Savage, P., 2017. The isotope geochemistry of zinc and copper.
619   Reviews in Mineralogy and Geochemistry, 82, 543-600.
620   Nakajima, M. and Stevenson, D.J., 2018. Inefficient volatile loss from the Moon-forming disk:
621   Reconciling the giant impact hypothesis and a wet Moon. Earth and Planetary Science Letters,
622   487, pp.117-126.
623   Neal, C.R., Taylor, L.A., 1992. Petrogenesis of mare basalts: A record of lunar volcanism.
624   Geochimica et Cosmochimica Acta, 56, 2177-2211.
625   Ni, P., Zhang, Y., Chen, S., Gagnon, J., 2019. A melt inclusion study on volatile abundances in
626   the lunar mantle. Geochimica et Cosmochimica Acta, 249, 17-41.

627 O'Neill, H.St.C., 1991. The origin of the Moon and the early history of the Earth – a chemical
628   model. Part 1: The Moon. Geochimica et Cosmochimica Acta, 55, 1135-1157.
629 Paniello, R.C., Day, J.M.D., Moynier, F., 2012a. Zinc isotopic evidence for the origin of the Moon.
630   Nature, 490, 376-379.
631 Paniello, R.C., Moynier, F., Beck, P., Barrat, J.A., Podosek, F.A., Pichat, S., 2012b. Zinc isotopes
632   in HEDs: Clues to the formation of 4-Vesta, and the unique composition of Pecora Escarpment
633   82502. Geochimica et Cosmochimica Acta, 86, 76-87.
634 Pringle, E.A., Moynier, F., 2017. Rubidium isotopic composition of the Earth, meteorites, and the
635   Moon: Evidence for the origin of volatile loss during planetary accretion. Earth and Planetary
636   Science Letters, 473, 62-70.
637 Rhodes, J.M., Hubbard, N.J., 1973. Chemistry, classification, and petrogenesis of Apollo 15 mare
638   basalts. Lunar and Planetary Science Conference Proceedings, 4, 1127-1147.
639 Sarafian, A.R., John, T., Roszjar, J., Whitehouse, M.J., 2017. Chlorine and hydrogen degassing in
640   Vesta's magma ocean. Earth and Planetary Science Letters, 459, 311-319.
641 Schnare, D.W., Day, J.M.D., Norman, M.D., Liu, Y., Taylor, L.A., 2008. A laser-ablation ICP-
642   MS study of Apollo 15 low-titanium olivine-normative and quartz-normative mare basalts.
643   Geochimica et Cosmochimica Acta, 72, 2556-2572.
644 Sedaghatpour, F., Jacobsen, S.B., 2019. Magnesium stable isotopes support the lunar magma
645   ocean cumulate remelting model for mare basalts. Proceedings of the National Academy of
646   Sciences, 116, 73-78.
647 Sharp, Z.D., Shearer, C.K., McKeegan, K.D., Barnes, J.D., Wang, Y.Q., 2010. The chlorine
648   isotope composition of the Moon and implications for an anhydrous mantle. Science, 329, 1050-
649   1053.
650 Shearer, C.K., Sharp, Z.D., Burger, P.V., McCubbin, F.M., Provencio, P.P., Brearley, A.J., Steele,
651   A., 2014. Chlorine distribution and its isotopic composition in "rusty rock" 66095. Implications
652   for volatile element enrichments of "rusty rock" and lunar soils, origin of "rusty" alteration, and
653   volatile element behavior on the Moon. Geochimica et Cosmochimica Acta 139, 411-433.
654 Shearer, C.K., Elardo, S.M., Petro, N.E., Borg, L.E., McCubbin, F.M., 2015. Origin of the lunar
655   highlands Mg-suite: An integrated petrology, geochemistry, chronology, and remote sensing
656   perspective. American Mineralogist, 100, 294-325.
657 Sossi, P.A., Nebel, O., O'Neill, H.S.C., Moynier, F., 2018. Zinc isotope composition of the Earth
658   and its behaviour during planetary accretion. Chemical Geology, 477, 73-84.
659 Sossi, P.A., Moynier, F., 2017. Chemical and isotopic kinship of iron in the Earth and Moon
660   deduced from the lunar Mg-Suite. Earth and Planetary Science Letters, 471, 125-135.
661 Snyder, G.A., Taylor, L.A., Neal, C.R., 1992. A chemical model for generating the sources of mare
662   basalts: Combined equilibrium and fractional crystallization of the lunar magmasphere.
663   Geochimica et Cosmochimica Acta, 56, 3809-3824.
664 Spicuzza, M.J., Day, J.M.D., Taylor, L.A., Valley, J.W., 2007. Oxygen isotope constraints on the
665   origin and differentiation of the Moon. Earth and Planetary Science Letters, 253, 254-265.
666 Taylor, S.R., Taylor, G.J., Taylor, L.A., 2006. The Moon: a Taylor perspective. Geochimica et
667   Cosmochimica Acta, 70, 5904-5918.
668 Urey, H.C., 1947, The thermodynamic properties of isotopic substances. Journal of the Chemical
669   Society (London), 562-581.
670 van Kooten, E.M.M.E., Moynier, F. 2019. Zinc isotope analyses of singularly small samples (< 5
671   ng Zn): investigating chondrule-matrix complementarity in Leoville. Geochimica et
672   Cosmochimica Acta, 261, 248-268.

673 Wang, K., Jacobsen, S.B., 2016. Potassium isotopic evidence for a high-energy giant impact origin
674   of the Moon. Nature, 538, 487-490.
675 Wang, Z.Z., Liu, S.A., Liu, J., Huang, J., Xiao, Y., Chu, Z.Y., Zhao, X.M. and Tang, L., 2017.
676   Zinc isotope fractionation during mantle melting and constraints on the Zn isotope composition
677   of Earth's upper mantle. Geochimica et Cosmochimica Acta, 198, pp.151-167.
678 Wang, X., Fitoussi, C., Bourdon, B., Fegley, B., Charnoz, S., 2019. Tin isotopes indicative of
679   liquid–vapour equilibration and separation in the Moon-forming disk. Nature Geoscience, 12,
680   707-711.
681 Warren, P.H., Wasson, J.T., 1979. The origin of KREEP. Reviews of Geophysics, 17(1), pp.73-
682   88.
683 Warren P.H., Wasson J.T., 1980. Further foraging of pristine nonmare rocks: Correlations between
684   geochemistry and longitude. Proc. 11th Lunar Planet. Sci. Conf. 431-470.
685 Wimpenny, J., Marks, N., Knight, K., Rolison, J.M., Borg, L., Eppich, G., Badro, J., Ryerson, F.J.,
686   Sanborn, M., Huyskens, M.H., Yin, Q.Z., 2019. Experimental Determination of Zn Isotope
687   Fractionation During Evaporative Loss at Extreme Temperatures. Geochimica et
688   Cosmochimica Acta, 259, 391-411.
689 Wolf, R., Anders, E., 1980. Moon and Earth: compositional differences inferred from siderophiles,
690   volatiles, and alkalis in basalts. Geochimica et Cosmochimica Acta, 44, 2111-2124.
691 Zhu, M.-H., Artemieva, N., Morbidelli, A., Yin, Q.-Z., Becker, H, Wünnemann, K. 2019.
692   Reconstructing the late accretion history of the Moon. Nature, 571, 226–229.

693   **Figures and Figure Captions**
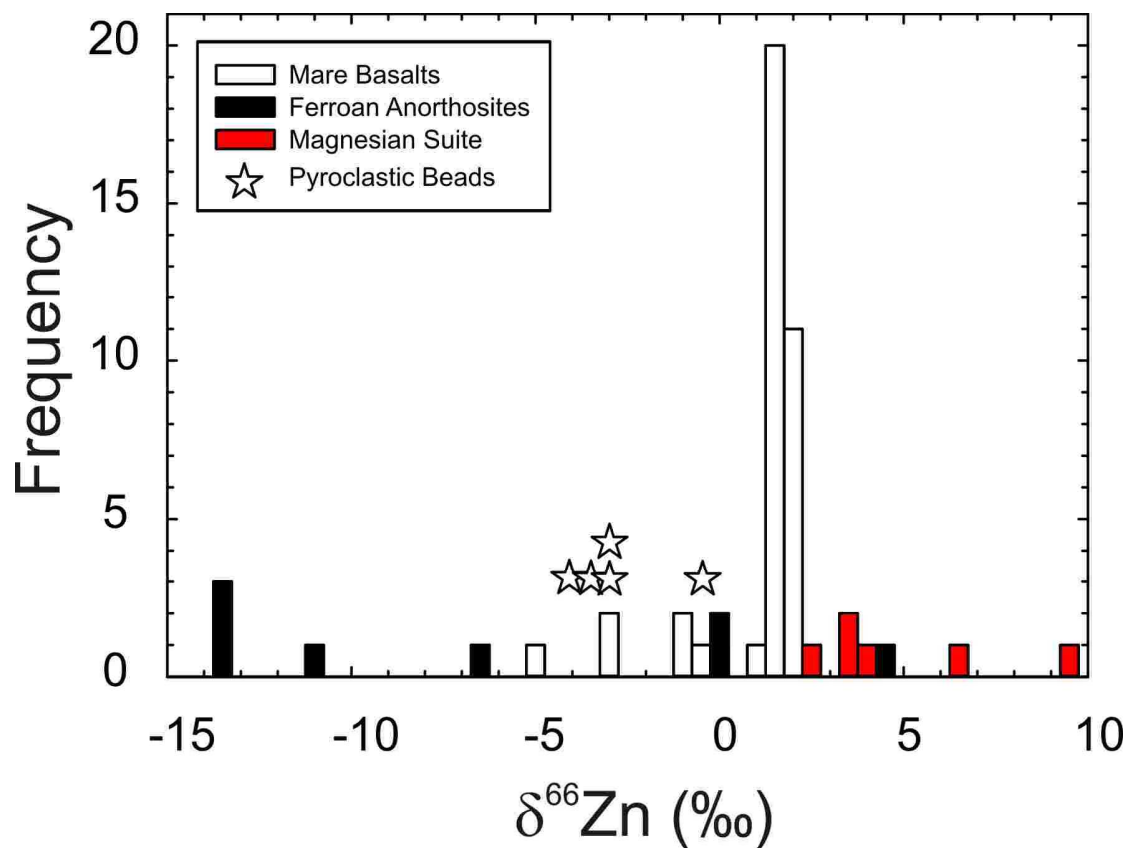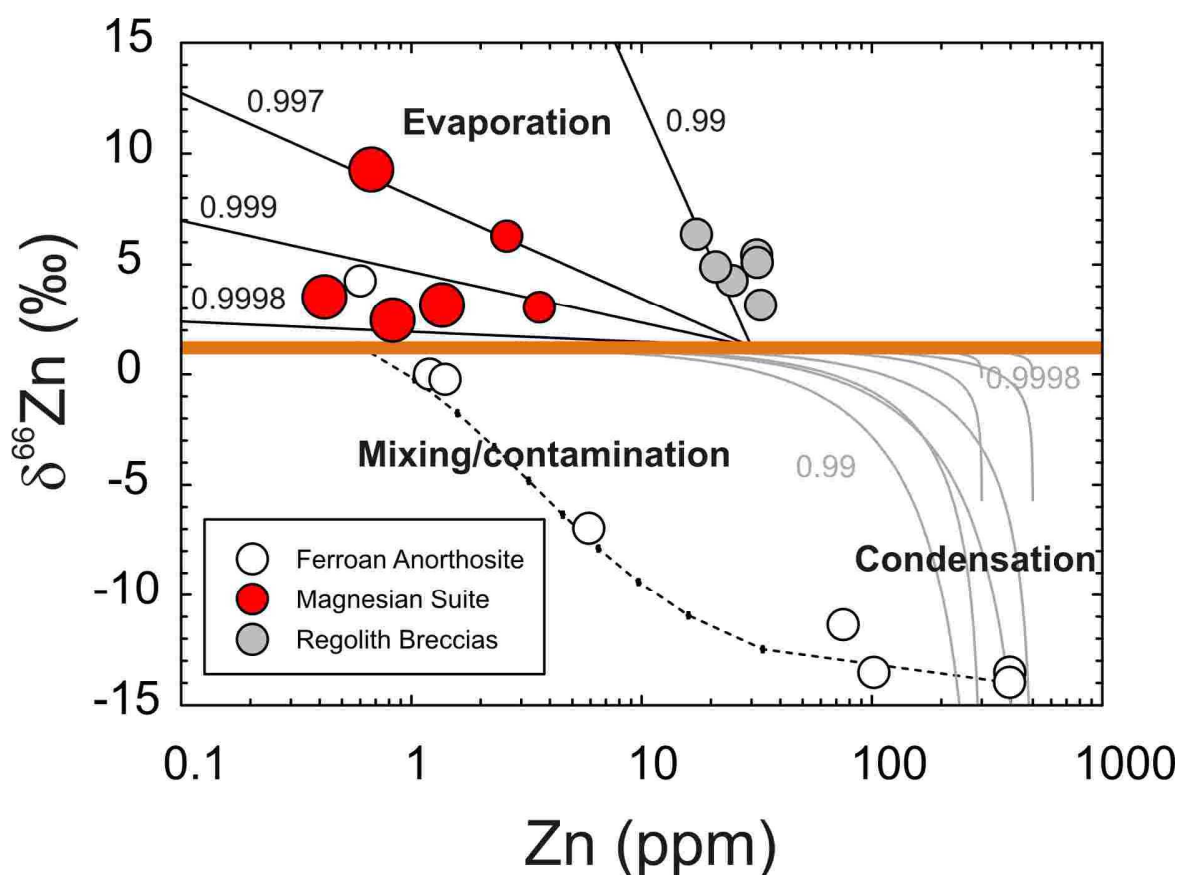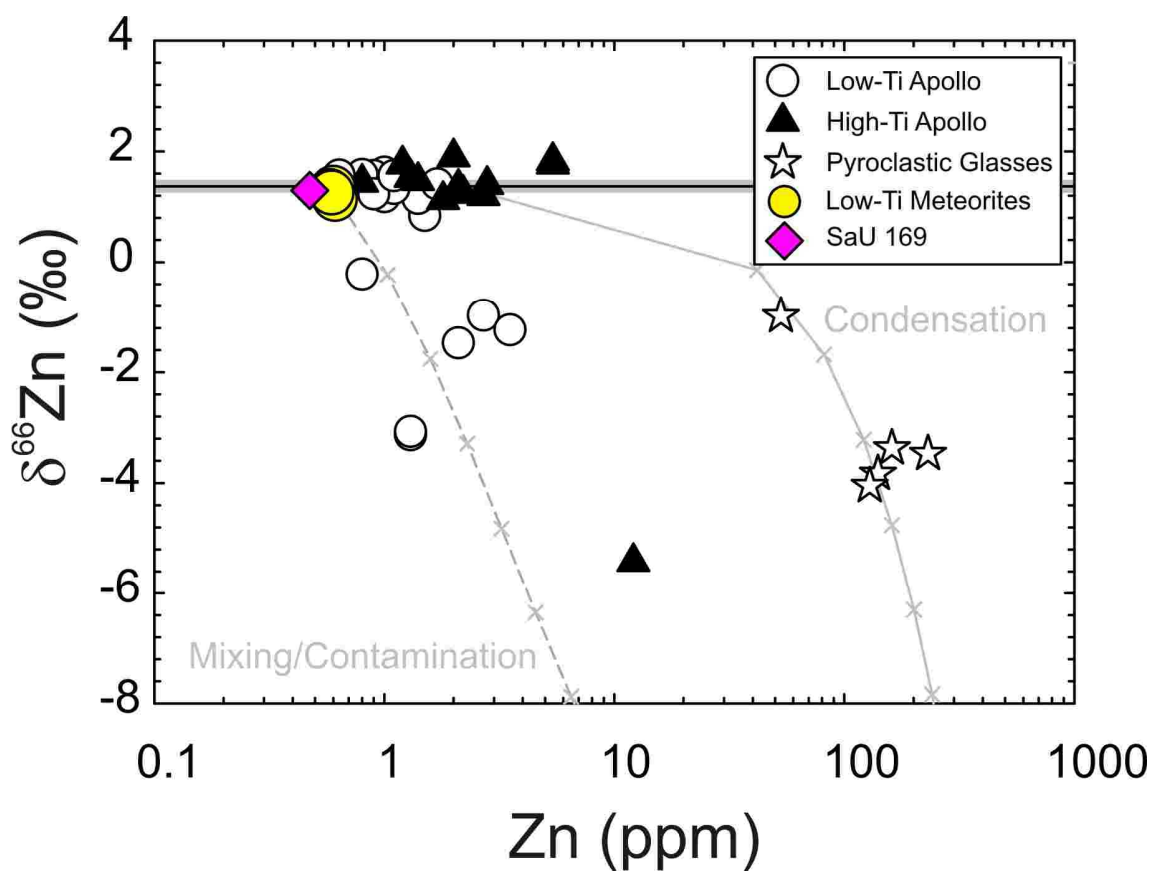
694

695

696   **Figure 1** – Histogram of zinc isotope compositions for lunar igneous samples. Data are from this
697   study (mare basalt meteorites and magnesian suite rocks), Moynier et al. (2006), Paniello et al.
698   (2012a) and Kato et al. (2015).

699

Figure 2 – Zinc isotope composition versus content for lunar crustal samples. Orange bar represents the estimated range in δ^{66}Zn for the mare basalt source, from Paniello et al. (2012a). Rayleigh distillation models of evaporation assume 30 ppm as the initial source composition, with fractionation factors (α) from Day et al. (2017b), to more extreme values. Condensation models represent sources with between 10-30 ppm initial Zn using the same fractionation factors. Mixing and contamination line in increments of 10% models the effect of adding a Zn composition observed in the 'Rusty Rock' 66095 with a pristine mare basalt composition and is after Day et al. (2017a). Large symbols represent new data from the study, with published data from Herzog et al. (2009), Kato et al., (2015) and Day et al. (2017a). Error bars are smaller than symbols.

Figure 3 - Zinc isotope composition versus content for mare basalts and pyroclastic glasses. Solid line and bar represent the estimated range in δ^{66}Zn for the mare basalt source, from **Table 2**. Condensation and mixing/contamination models are the same as those calculated from Day et al. (2017a) and Figure 2. Data are from this study (Low-Ti mare basalt meteorites and SaU 169), Paniello et al. (2012a) and Kato et al. (2015). Error bars are smaller than symbols.
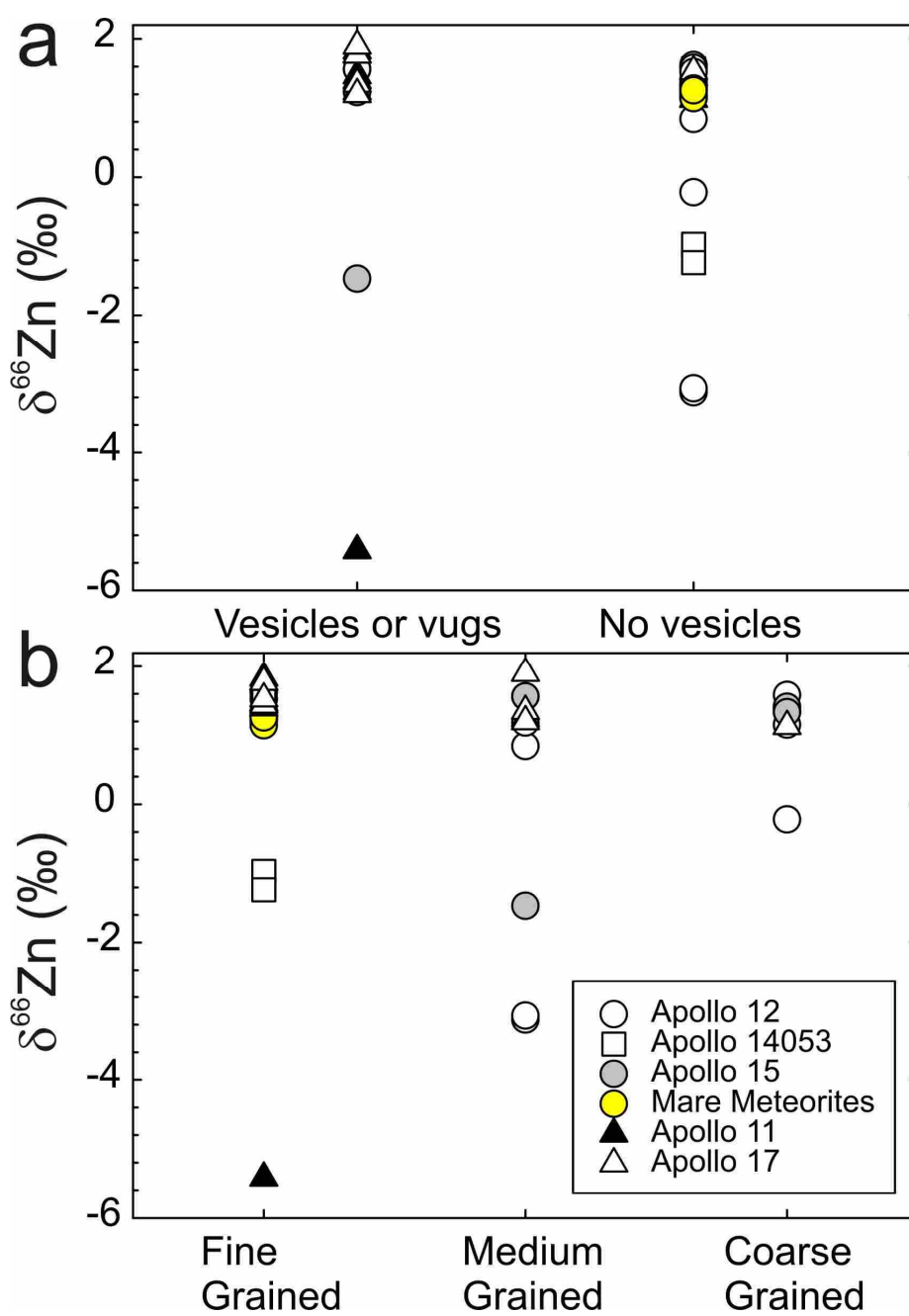
Figure 4 – Relationships of δ⁶⁶Zn for (a) vesiculated or vuggy versus non-vesicular mare basalts and (b) versus mare basalt grain size. Data are given in **Table S1**.
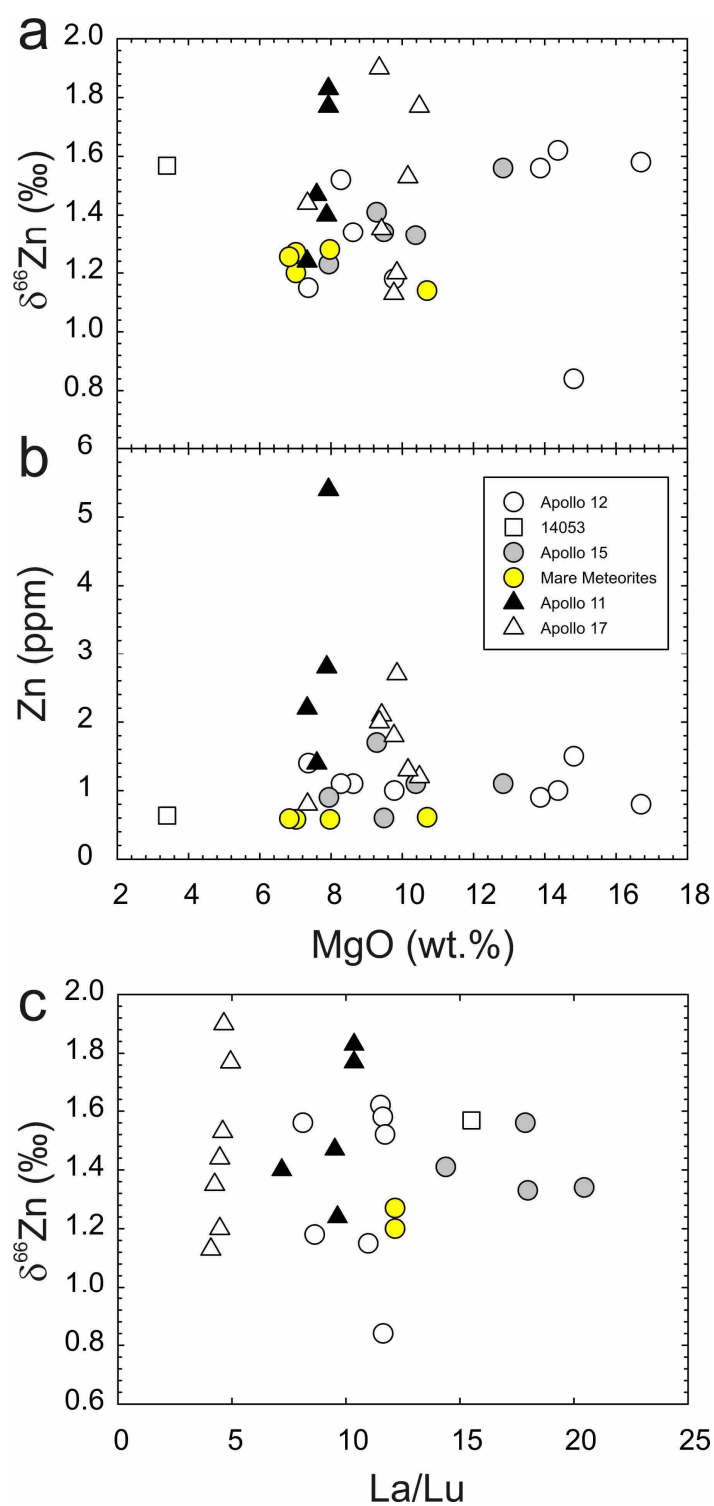
Figure 5 – Zinc isotope compositions (a) and abundances (b) for lunar mare basalts as a function of MgO content, and Zn isotopes versus La/Lu (c). Data for Zn are from this study, Paniello et al. (2012a), Kato et al. (2015), and for MgO content and La/Lu are from the lunar compendium and reported in **Table S1**. Error bars are smaller than symbols.
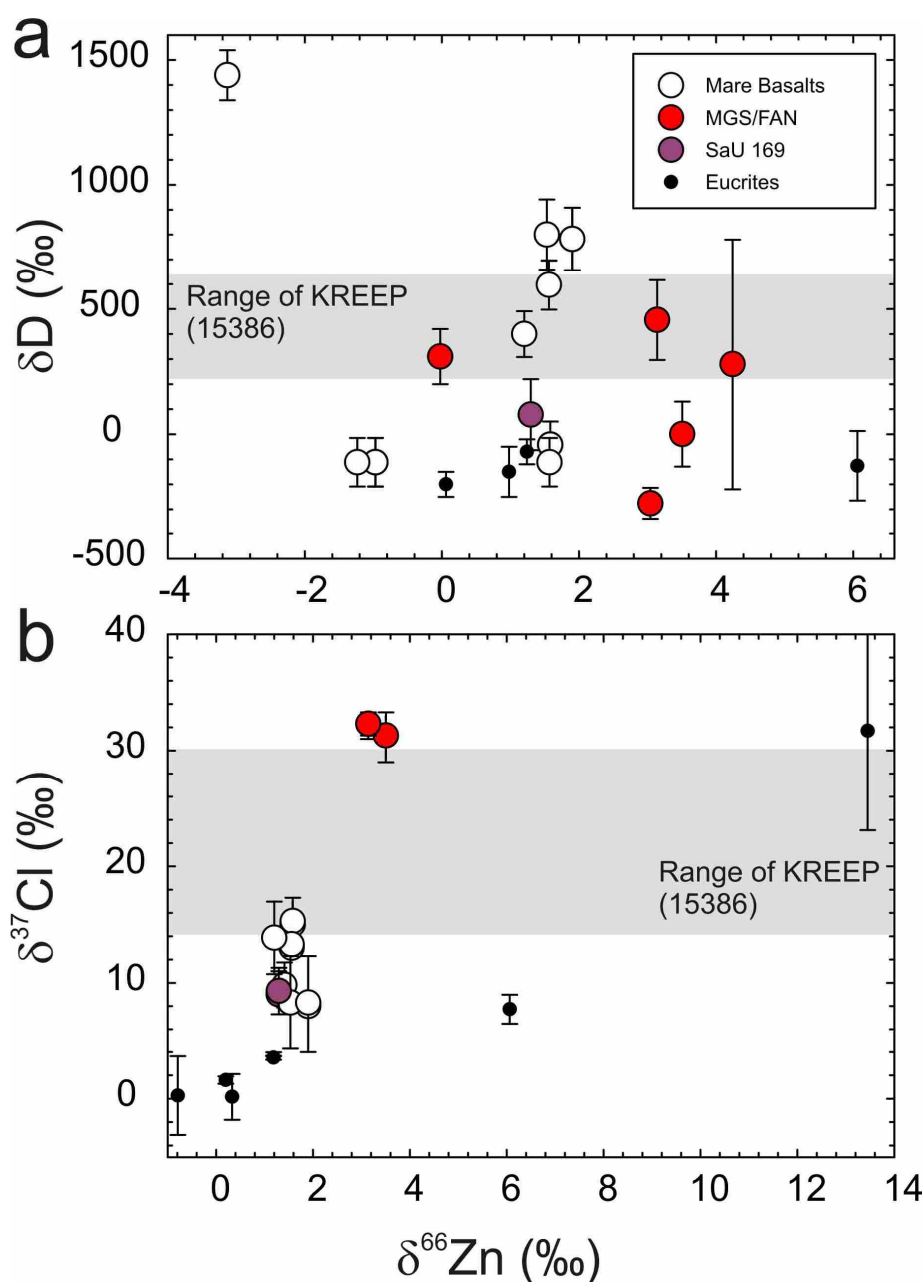
724

Figure 6 – Plots of (a) hydrogen and (b) chlorine versus zinc isotope composition for lunar samples
and eucrite meteorites. Gray bar represents the hydrogen and chlorine isotope composition of
KREEP basalt 15386; Zn isotope data has not been obtained for this sample. Zinc isotope data
sources are the same as those for Figure 2, with lunar hydrogen and chlorine isotope data from the
compilation in McCubbin et al. (2015), and H, Cl and Zn isotope data for eucrites from Paniello
et al. (2012b), Sarafian et al. (2017) and Barrett et al. (2019) and reported in **Table S2**. Error bars
are smaller than symbols, unless they are shown.

732

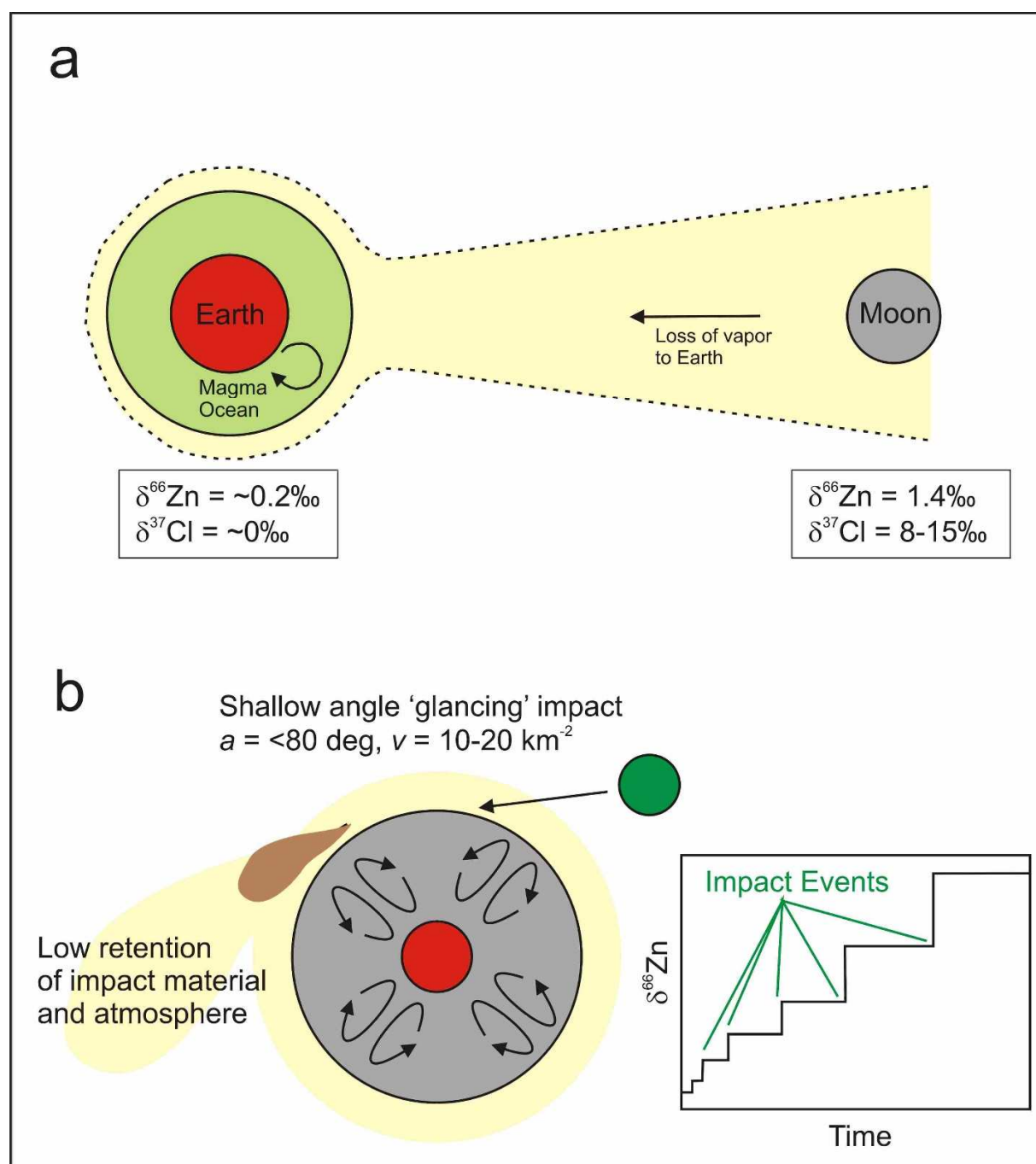**Figure 7** – Scenarios to explain the δ^{66}Zn and δ^{37}Cl of mare basalt mantle sources. In (a) the giant impact that created the Earth and Moon leads to volatile loss from the Moon, possibly to Earth or to space, resulting in a dichotomy in moderately volatile element abundances and isotopic compositions (c.f., Lock et al., 2018). In (b) impact erosion from glancing impacts to the Moon (cf. Zhu et al., 2019) lead to loss of impactor mass and of volatile elements. Multiple impacts result in progressive depletion in the volatile elements and preferential enrichment in the heavier isotopes of zinc (inset schematic).

Table 1: Zinc isotopes and abundances in mare basalt meteorites and Mg-suite rocks

Sample		Type	Zn ppm	δ^{66}Zn	2SD	δ^{66}Zn	2SD	δ^{66}Zn	2SD
78235, 156	Mg-Suite	Shocked Norite		3.40		5.30		6.90	
				3.61		5.66		7.3	
		Average	**0.42**	**3.51**	**0.30**	**5.48**	**0.51**	**7.10**	**0.57**
15455, 391	Mg-Suite	Norite CAN clast		9.23		14.27		18.74	
				9.31		14.52		18.89	
		Average	**0.67**	**9.27**	**0.11**	**14.40**	**0.35**	**18.82**	**0.21**
15445, 333	Mg-Suite	Norite (Clast B)		2.25		3.92		5.09	
				2.66		4.46		5.7	
		Average	**0.83**	**2.46**	**0.58**	**4.19**	**0.76**	**5.40**	**0.86**
76535, 186	Mg-Suite	Troctolite	**1.36**	**3.14**		**5.03**		**6.58**	
SAU 169	KREEP	Impact Melt		1.31		2.05		2.62	
		Breccia		1.28		1.91		2.52	
		Average	**0.47**	**1.30**	**0.04**	**1.98**	**0.20**	**2.57**	**0.14**
LAP 02205	Low-Ti Mare	Meteorite		1.28		1.76		2.56	
				1.26		1.98		2.56	
				1.27		1.86		2.55	
		Average	**0.58**	**1.27**	**0.02**	**1.87**	**0.22**	**2.56**	**0.01**
NWA 8632	Low-Ti Mare	Meteorite		1.16		1.65		2.39	
				1.12		1.69		2.23	
		Average	**0.61**	**1.14**	**0.06**	**1.67**	**0.06**	**2.31**	**0.23**
NWA 479	Low-Ti Mare	Meteorite		1.33		1.94		2.59	
				1.24		1.88		2.45	
				1.27		1.94		2.47	
		Average	**0.58**	**1.28**	**0.09**	**1.92**	**0.07**	**2.50**	**0.15**
NWA 4734	Low-Ti Mare	Meteorite		1.23		2.11		2.5	
				1.28		2.28		2.51	
		Average	**0.59**	**1.26**	**0.07**	**2.20**	**0.24**	**2.51**	**0.01**

Table 2: Zinc reservoir compositions in and on the Moon

	Zn ppm	2SE	δ^{66}Zn	2SE	n
Low-Ti Apollo Source(s)	1.1	0.2	1.37	0.12	14
Low-Ti Mare Meteorites	0.59	0.01	1.23	0.05	5
High-Ti Apollo Source(s)	2.4	0.9	1.50	0.15	12
Mare Sources			*1.40*	*0.20*	
KREEP	0.47	-	>1.3	-	1
Pristine FAN	0.60	-	>4	-	1
Mg-Suite	0.67	-	2.4 to 9.3	-	1
Condensate	300	100	-13.7	0.3	3
Impact Gardened Material	27	5	5.1	0.9	7